Supplement of Geosci. Model Dev., 16, 2261–2276, 2023
https://doi.org/10.5194/gmd-16-2261-2023-supplement

Geoscientific Model Development
Open Access

Supplement of

Implementation of trait-based ozone plant sensitivity in the Yale Interactive terrestrial Biosphere model v1.0 to assess global vegetation damage

Yimian Ma et al.

Correspondence to: Xu Yue (yuexu@nuist.edu.cn) and Stephen Sitch (s.a.sitch@exeter.ac.uk)

Table S1. Data for calibration. Each S_O (% per mmol m^{-2}) value is derived as the slope of regression between the corresponding O$_3$ metric (ϕ_{O3}) and biotic indicator (R) in Equation (5).

PFT	Reference	Species	Regions	ϕ_{O3}	*D*	S_O	Sub-references
EBF (median S_O: -0.19)	Clrtap (2017) Figure III.12	Quercus ilex L.	Spain	$POD_{y=1}$	Above-ground biomass	-0.09	Alonso et al. (2014)
	Assis et al. (2015)	Psidium guajava L. 'Paluma'	Brazil	$POD_{y=1}$	Leaf injury index	-0.19 -0.05 -0.2 -0.58	
NF (median S_O: -0.23)	Clrtap (2017) Figure III.12	Picea abies	France, Sweden, Switzerland	$POD_{y=1}$	Total biomass	-0.22	Buker et al. (2015)
	Feng et al. (2018)	Picea abies, Pinus halepensis, Pinus sylvestris	Europe	$POD_{y=1}$	Total biomass	-0.24	Elvira et al. (2007); Karlsson et al. (2004); Ottosson et al. (2003); Alonso et al. (2003); Medlyn et al. (1999); Braun and Fluckiger (1995)
DBF (median S_O: -0.70)	Clrtap (2017) Figure III.12	Fagus sylvatica, Betula pendula	Finland, Sweden, Switzerland	$POD_{y=1}$	Total biomass	-0.93	Buker et al. (2015)
	Clrtap (2017) Figure III.12	Quercus faginea; Q. pyrenaica，Q. robur	Italy, Spain	$POD_{y=1}$	Total biomass	-0.32	Calatayud et al. (2011); Marzuoli et al. (2016)
	Buker et al. (2015) Supplementary data	Betula pendula Quercus roburor	Europe	$POD_{y=1}$	Total biomass	-0.61	Uddling et al. (2004); Ottosson et al. (2003); Dixon et al. (1998); Karlsson et al. (2003)
	Hoshika et al. (2018)	Quercus pubescens, Q. robur	Italy	$POD_{y=1}$	Total biomass	-0.73, -1.4	
	Marzuoli et al. (2018)	Quercus pyrenaica, Q. faginea，Q. robur	Spain,Italy	$POD_{y=1}$ $POD_{y=1}$	Total biomass Total biomass	-0.32, -0.52	
	Hu et al. (2015)	Poplar (5 clones)	China	$POD_{y=1}$	Total biomass	-0.75	
GRA_C4 (median S_O: -0.85)	Clrtap (2017) Figure III.14	Mediterranean pasture	Spain	$POD_{y=1}$	Above-ground biomass	-0.85	Gimeno et al. (2004a); Gimeno et al. (2004b); Sanz et al. (2005); Sanz et al. (2007); Sanz

							et al. (2014); Sanz et al. (2016)
GRA_C3 (median S_O: -0.62)	Clrtap (2017) Figure III.13	Temperate grassland	UK	$POD_{y=1}$	Total biomass	-0.62	Hayes et al. (2011); Hayes et al. (2012) Wyness et al. (2011); Wagg et al. (2012); Hewitt et al. (2014)
CRO (median S_O: -3.35)	Peng et al. (2020)	Maize (2 varieties)	China	$POD_{y=6}$ $POD_{y=6}$	Total biomass Total biomass	-5.26 -3.32	
	Peng et al. (2019)	Maize	China	$POD_{y=6}$	Total biomass	-4.26	
	Hayes et al. (2020)	Bean, Cowpea (13 varieties)	Africa	$POD_{y=6}$ $POD_{y=6}$	Yield Thousand grain weight	-2.58 -1.2	
	Hayes et al. (2020)	Wheat	Africa	$POD_{y=6}$ $POD_{y=6}$	Yield Thousand grain weight	-3.5 -2.9	
	Clrtap (2017) Figure III.10	Wheat	Synthesis	$POD_{y=6}$	Grain yield	-3.85	
	Clrtap (2017) Figure III.10	Wheat	Synthesis	$POD_{y=6}$	1000 grain yield	-3.35	
	Clrtap (2017) Figure III.10	Wheat	Synthesis	$POD_{y=6}$	Protein production	-2.54	
	Clrtap (2017) Figure III.11	Tomato	Synthesis	$POD_{y=6}$	Yield	-2.53	
	Clrtap (2017) Table III.10	Tomato	Synthesis	$POD_{y=6}$	Fruit yield	-2.66	
	Zhang et al. (2017)	Soybean	China	$POD_{y=6}$	Seed yield	-3.3	
	Harmens et al. (2018)	Wheat (2 varieties)	Europe	$POD_{y=6}$ $POD_{y=6}$ $POD_{y=6}$ $POD_{y=6}$	Yield Yield 1000 grain weight 1000 grain weight	-3.9 -6.5 -3.4 -4.8	

Table S2. PFT-specific LMA for the YIBs-LMA_PFT [a] experiment.

PFT	EBF	NF	DBF	C_SHR	A_SHR	C4_GRA	C3_GRA	CRO
LMA [b] (g m^{-2})	83.9	158.1	53.9	68.8	68.8	47.7	47.7	47.7
Source types [c]	EBF	ENF, DNF	DBF	SHL	SHL	GRL	GRL	GRL

[a] The YIBs-LMA_PFT experiment uses x=0.019 nmol g^{-1} s^{-1} and PFT-specific LMA from M2018, which is different from YIBs-LMA in the way of LMA assignment. Details are summarized in Table 1.

[b] The average LMA for certain PFT is calculated from M2018 dataset.

[c] For each PFT in the YIBs model, the vegetation types from original paper of M2018 are listed, including EBF, ENF, DNF (Deciduous needleleaf forest), DBF, SHL (shrubland), and GRL (grassland).

Table S3. Calibrations of the YIBs-LMA_PFT [a] experiment with varied *a*.

PFT	S_O	S_S					S_S/S_O [b]				
		a=2.0	a=2.5	a=3.0	a=3.5	a=4.0	**a=2.0**	a=2.5	a=3.0	a=3.5	a=4.0
EBF	-0.19	**-0.14**	-0.18	-0.21	-0.25	-0.28	**0.76**	0.95	1.13	1.30	1.48
NF	-0.23	**-0.07**	-0.09	-0.11	-0.12	-0.14	**0.32 ***	0.4 *	0.47 *	0.54 *	0.61 *
DBF	-0.70	**-0.63**	-0.78	-0.92	-1.07	-1.21	**0.90**	1.11	1.32	1.53	1.73
C_SHR	/	**-0.72**	-0.90	-1.07	-1.24	-1.41	/	/	/	/	/
A_SHR	/	**-0.39**	-0.48	-0.58	-0.67	-0.76	/	/	/	/	/
C4_GRA	-0.85	**-0.92**	-1.15	-1.37	-1.59	-1.81	**1.09**	1.35	1.61	1.87	2.13
C3_GRA	-0.62	**-0.68**	-0.84	-1.00	-1.17	-1.33	**1.09**	1.36	1.62	1.88	2.14
CRO	-3.35	**-3.34**	-5.05	-7.51	-11.21	-17.08	**1.00**	1.51	2.24	3.35	5.10
Fitting [c]	/	**1.00**	1.47	2.14	3.13	4.69	/	/	/	/	/
Median	/	/	/	/	/	/	**0.95 (1.00)**	1.23 (1.35)	1.47 (1.61)	1.70 (1.87)	1.93 (2.13)
Std	/	/	/	/	/	/	**0.29 (0.14)**	0.4 (0.22)	0.59 (0.42)	0.93 (0.80)	1.53 (1.47)

[a] All tests of the YIBs-LMA_PFT experiment use x=0.019 nmol g^{-1} s^{-1} and PFT-specific LMA information from M2018 (Table S2), which is different from YIBs-LMA in the way of LMA assignment.

[b] Slopes of simulated PFT-specific DRRs (S_S) are divided by observations (S_O, Table S1) to derive the model-to-observation ratios (S_S/S_O). O_3 dose metric is $POD_{y=1}$ for natural PFTs and $POD_{y=6}$ for crops. The Median and standard deviation (Std) of S_S/S_O ratios of all PFTs are calculated for each set of specific parameter *a*. The values in parentheses exclude the effect of those numbers marked with * that are out of 1 standard deviation.

[c] The slopes (Fitting) of linear regressions between S_O and S_S are listed for each *a*. The optimal *a* with 1:1 fitting between S_S and S_O is bolded.

Table S4. Calibrations of the YIBs-LMA_T [a] experiment with varied *a*.

PFT	S_O	S_S					S_S/S_O [b]				
		a=2.0	a=2.5	**a=3.0**	a=3.5	a=4.0	a=2.0	a=2.5	**a=3.0**	a=3.5	a=4.0
EBF	-0.19	-0.21	-0.26	**-0.31**	-0.36	-0.41	1.08	1.35	**1.62**	1.89	2.16
NF	-0.23	-0.33	-0.41	**-0.49**	-0.57	-0.65	1.43	1.78	**2.14**	2.49	2.84
DBF	-0.70	-0.50	-0.63	**-0.75**	-0.87	-0.99	0.72	0.90	**1.07**	1.25	1.42
C_SHR	/	-1.10	-1.38	**-1.66**	-1.94	-2.23	/	/	/	/	/
A_SHR	/	-0.44	-0.55	**-0.67**	-0.78	-0.89	/	/	/	/	/
C4_GRA	-0.85	-0.87	-1.09	**-1.31**	-1.53	-1.76	1.02	1.28	**1.54**	1.80	2.07
C3_GRA	-0.62	-0.49	-0.61	**-0.73**	-0.85	-0.98	0.79	0.98	**1.18**	1.38	1.57
CRO	-3.35	-1.72	-2.38	**-3.19**	-4.19	-5.43	0.51	0.71	**0.95**	1.25	1.62
Fitting [c]	/	0.56	0.76	**1.00**	1.29	1.64	/	/	/	/	/
Median	/	/	/	/	/	/	0.91	1.13	**1.36**	1.59	1.84
Std	/	/	/	/	/	/	0.32	0.39	**0.44**	0.49	0.53

[a] All tests from the YIBs-LMA_T experiment use the threshold x=0.006 nmol g^{-1} s^{-1} and the gridded LMA from of M2018 map. Details are summarized in Table 1.
[b] Slopes of simulated PFT-specific DRR (S_S) are divided by observations (S_O, Table S1) to derive the model-to-observation ratios (S_S/S_O). O_3 dose metric is $POD_{y=1}$ for natural PFTs and $POD_{y=6}$ for crops. The Median and standard deviation (Std) of S_S/S_O ratios of all PFTs are calculated for each set of specific parameter *a*.
[c] The slopes (Fitting) of linear regressions between S_O and S_S are listed for each *a*. The optimal *a* with 1:1 fitting between S_S and S_O is bolded.

Table S5. Calibrations of the YIBs-LMA_B2017 [a] experiment with varied *a*.

PFT	S_O	S_S					S_S/S_O [b]				
		a=2.0	a=2.5	**a=2.8**	a=3.0	a=3.5	a=2.0	a=2.5	**a=2.8**	a=3.0	a=3.5
EBF	-0.19	-0.16	-0.19	**-0.22**	-0.23	-0.27	0.82	1.02	**1.14**	1.21	1.40
NF	-0.23	-0.24	-0.29	**-0.33**	-0.35	-0.40	1.04	1.28	**1.43**	1.51	1.73
DBF	-0.70	-0.51	-0.63	**-0.70**	-0.74	-0.86	0.73	0.90	**1.00**	1.06	1.23
C_SHR	/	-1.22	-1.51	**-1.69**	-1.79	-2.07	/	/	**/**	/	/
A_SHR	/	-0.36	-0.45	**-0.50**	-0.53	-0.61	/	/	**/**	/	/
C4_GRA	-0.85	-0.79	-0.97	**-1.09**	-1.16	-1.34	0.92	1.15	**1.29**	1.36	1.58
C3_GRA	-0.62	-0.58	-0.72	**-0.80**	-0.85	-0.99	0.93	1.15	**1.30**	1.37	1.59
CRO	-3.35	-1.97	-2.67	**-3.17**	-3.46	-4.35	0.59	0.80	**0.94**	1.03	1.30
Fitting [c]	/	0.62	0.83	**0.98**	1.07	1.32	/	/	**/**	/	/
Median	/	/	/	**/**	/	/	0.87	1.08	**1.22**	1.29	1.49
Std	/	/	/	**/**	/	/	0.16	0.18	**0.19**	0.19	0.19

[a] All tests of the YIBs-LMA_map experiment use the same threshold x=0.019 nmol g^{-1} s^{-1} as YIBs-LMA, but gridded LMA information from another LMA map of B2017. Details are summarized in Table 1.

[b] Slopes of simulated PFT-specific DRR (S_S) are divided by observations (S_O, Table S1) to derive the model-to-observation ratios (S_S/S_O). O_3 dose metric is $POD_{y=1}$ for natural PFTs and $POD_{y=6}$ for crops. The Median and standard deviation (Std) of S_S/S_O ratios of all PFTs are calculated for each setting of specific parameter *a*.

[c] The slopes (Fitting) of linear regressions between S_O and S_S are listed for each *a*. The optimal *a* with 1:1 fitting between S_S and S_O is bolded.

Table S6. PFT-specific a_{PFT} and y for YIBs-S2007_adj [a] experiment.

PFT	EBF	NF	DBF	C_SHR [c]	A_SHR [d]	C4_GRA	C3_GRA	CRO
a_{PFT} ($nmol^{-1}$ m^2 s)	0.023	0.017	0.042	0.015	0.030	0.041	0.041	0.039
y (nmol m^{-2} s^{-1}) [b]	1	1	1	1	1	1	1	1

[a] YIBs-S2007_adj adopts area-based flux expression in S2007. The sensitivity parameter a_{PFT} are recalibrated according to S_O in Table S1. Details are summarized in Table 1.

[b] The thresholds y are set to 1 nmol m^{-2} s^{-1} for all PFTs according to Oliver et al. (2018).

[c] S_O for calibrating C_SHR is assumed as the mean of EBF and DBF in Table S1.

[d] S_O for calibrating A_SHR is assumed as the mean of EBF and DBF in Table S1.

Table S7. Key parameters for the vegetation model. Maximum carboxylation capacity (μmol m^{-2} s^{-1}) at 25 degrees Celsius, leaf nitrogen content (g m^{-2}).

PFT	EBF	NF	DBF	C_SHB	A_SHB	C4_GRA	C3_GRA	CRO
Vcmax25 (μmol m^{-2} s^{-1})	29.0	50.8	59.6	57.9	57.9	24.0	78.2	100.7
Nleaf (g m^{-2})	2.17	2.46	1.80	1.86	1.86	1.32	1.75	1.62

Table S8. Summary of O_3 vegetation damages. GPP of each PFT (GPP_{PFT}, Pg C year^{-1}), absolute GPP changes of each PFT (ΔGPP_{PFT}, Pg C year^{-1}), relative GPP changes of each PFT ($\Delta GPP_{PFT}/GPP_{PFT}$, %), ratio of PFT-level GPP changes to global GPP ($\Delta GPP_{PFT}/GPP$, %).

Simulations[a]		**EBF**	**ENF**	**DBF**	**C_SHR**	**A_SHR**	**CRA_C4**	**GRA_C3**	**CRO**	**Total**
No O_3	GPP_{PFT}	29.72	19.04	8.96	4.02	21.57	20.84	25.92	17.60	147.65
YIBs-LMA	GPP_{PFT}	29.40	18.61	8.48	3.95	20.63	20.05	24.03	15.39	140.54
	ΔGPP_{PFT}	-0.31	-0.43	-0.47	-0.07	-0.93	-0.79	-1.89	-2.21	-7.11
	$\Delta GPP_{PFT}/GPP_{PFT}$	-1.05	-2.25	-5.27	-1.86	-4.33	-3.79	-7.28	-12.56	\
	$\Delta GPP_{PFT}/GPP$	-0.21	-0.29	-0.32	-0.05	-0.63	-0.53	-1.28	-1.50	-4.81
YIBs-LMA_PFT	GPP_{PFT}	29.48	18.97	8.45	3.96	20.89	19.96	23.85	15.23	140.79
	ΔGPP_{PFT}	-0.24	-0.07	-0.50	-0.06	-0.68	-0.89	-2.07	-2.37	-6.86
	$\Delta GPP_{PFT}/GPP_{PFT}$	-0.80	-0.36	-5.61	-1.45	-3.13	-4.25	-7.98	-13.45	\
	$\Delta GPP_{PFT}/GPP$	-0.16	-0.05	-0.34	-0.04	-0.46	-0.60	-1.40	-1.60	-4.65
YIBs-LMA_T	GPP_{PFT}	28.95	18.32	8.33	3.86	20.26	19.62	23.62	15.13	138.08
	ΔGPP_{PFT}	-0.76	-0.72	-0.63	-0.16	-1.31	-1.22	-2.29	-2.47	-9.56
	$\Delta GPP_{PFT}/GPP_{PFT}$	-2.57	-3.80	-7.00	-3.88	-6.08	-5.85	-8.85	-14.03	\
	$\Delta GPP_{PFT}/GPP$	-0.52	-0.49	-0.42	-0.11	-0.89	-0.83	-1.55	-1.67	-6.48
YIBs-LMA_B2017	GPP_{PFT}	29.28	18.60	8.46	3.88	20.62	19.97	23.76	15.27	139.85
	ΔGPP_{PFT}	-0.44	-0.44	-0.49	-0.14	-0.94	-0.87	-2.15	-2.32	-7.80
	$\Delta GPP_{PFT}/GPP_{PFT}$	-1.47	-2.30	-5.52	-3.45	-4.38	-4.18	-8.31	-13.19	\
	$\Delta GPP_{PFT}/GPP$	-0.30	-0.30	-0.33	-0.09	-0.64	-0.59	-1.46	-1.57	-5.28
YIBs-S2007_adj	GPP_{PFT}	29.32	18.75	8.39	3.98	20.76	20.02	23.95	15.41	140.58
	ΔGPP_{PFT}	-0.39	-0.29	-0.56	-0.04	-0.81	-0.82	-1.97	-2.19	-7.07
	$\Delta GPP_{PFT}/GPP_{PFT}$	-1.32	-1.53	-6.28	-1.02	-3.75	-3.92	-7.60	-12.44	\
	$\Delta GPP_{PFT}/GPP$	-0.27	-0.20	-0.38	-0.03	-0.55	-0.55	-1.33	-1.48	-4.79

[a] All results utilize optimal parameters shown in Table 1.

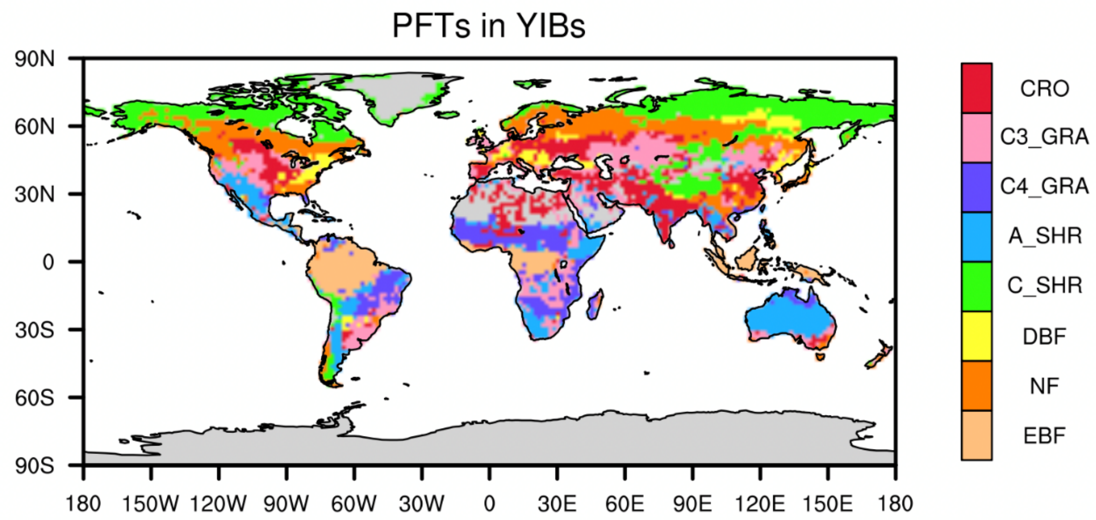

Figure S1. Dominant plant functional types (PFTs) in YIBs model. The PFTs include evergreen broadleaf forest (EBF), needleleaf forest (NF), deciduous broadleaf forest (DBF), arid/cold shrubland (A_SHR/C_SHR), C_3/C_4 grassland (C3_GRA/C4_GRA), and cropland (CRO).

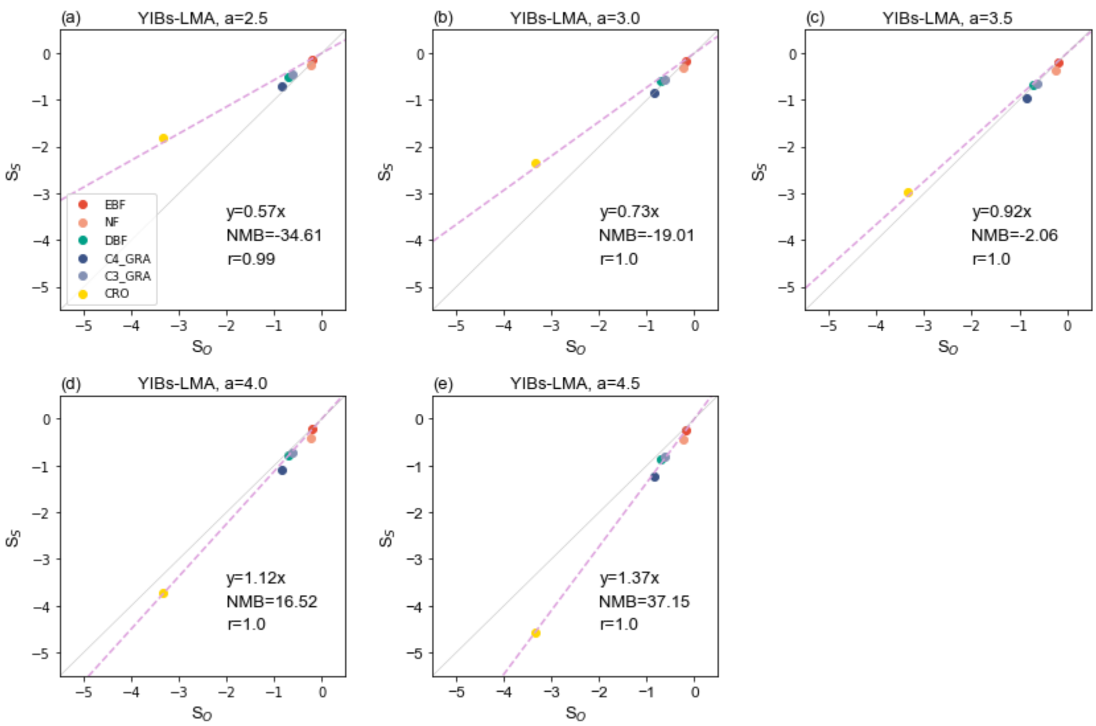

Figure S2. The calibration and validation with O_3 data in the year 2020 from CMIP6 SSP5-8.5 scenario. The forcing data remains the same as YIBs-LMA and calibration procedures are the same as in Fig 3. The new calibration achieved a minor shift of the optimal *a* from 3.5 to 3.6.

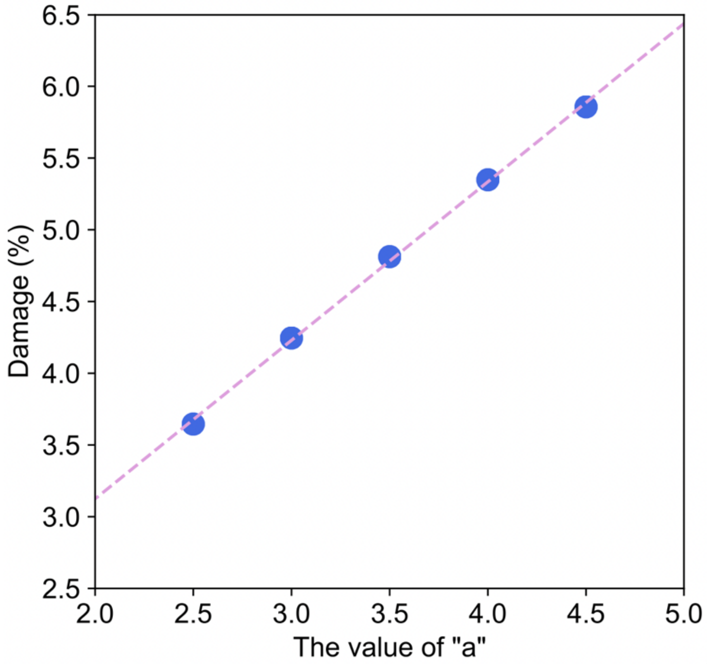

Figure S3. Derived O_3 damage percentages of global GPP (Damage, %) with varied parameter *a* for the YIBs-LMA experiment. The YIBs-LMA experiment is described in Section 2.3 and Table 1.

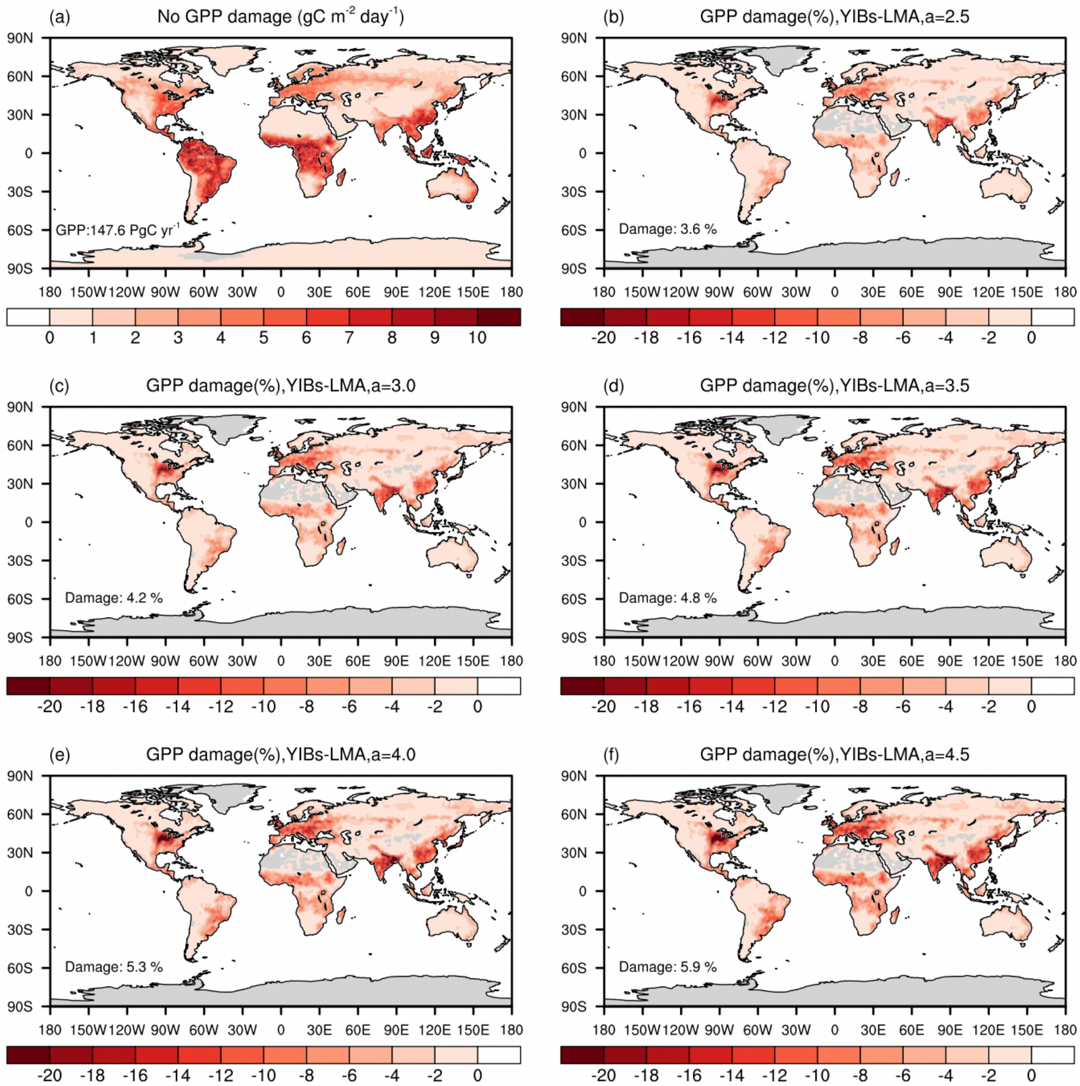

Figure S4. Global distribution of (a) GPP and (b-f) its damage percentages by O_3 with different parameter *a* for the YIBs-LMA experiment. The global total GPP is shown in (a) and the average damage percentages are shown in (b-f). The YIBs-LMA experiment is described in Table 1.

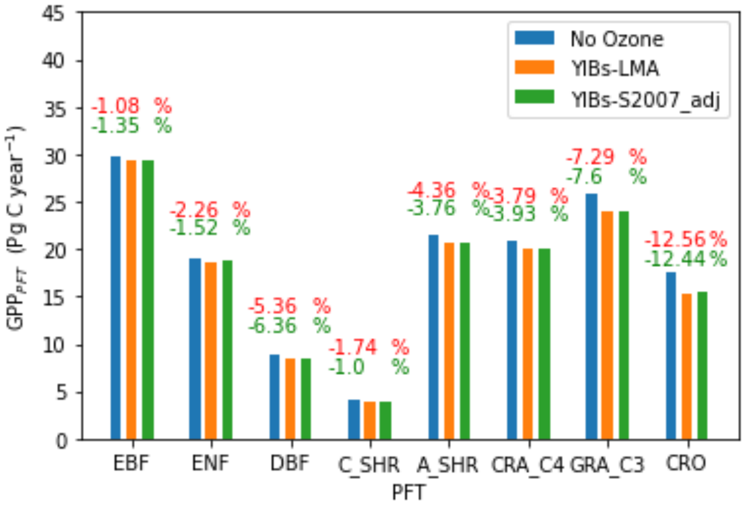

Figure S5. Comparison of PFT-specific GPPs from YIBs-LMA and YIBs-S2007_adj. Data for each PFT are shown as bars with blue, red, and green representing different experiments. Ratio numbers above each group of bars reveal the PFT-specific damage ratios for simulations using two schemes with red and green representing YIBs-LMA and YIBs-S2007_adj, respectively.

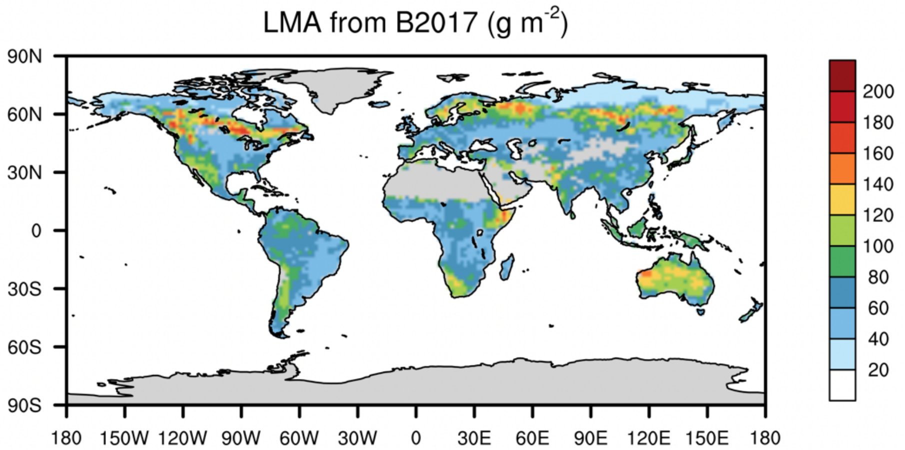

Figure S6. Distribution of LMA from B2017.

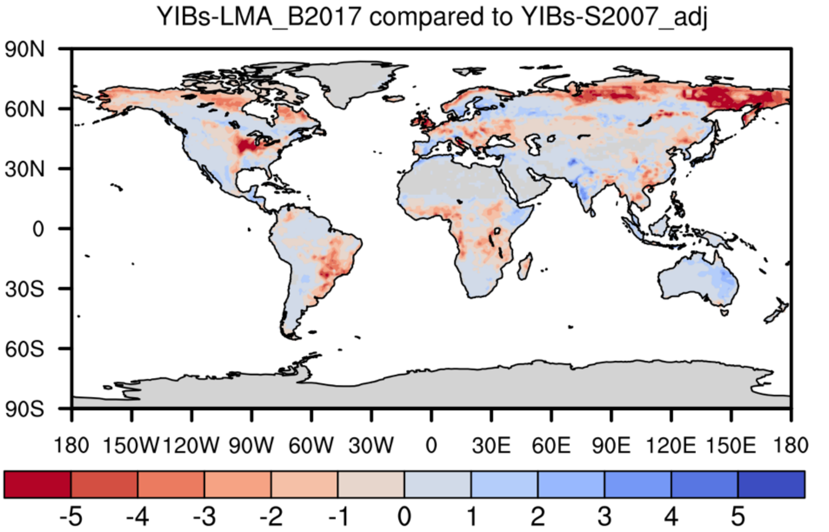

Figure S7. Differences between global O_3 vegetation damage map from the YIBs-LMA_B2017 experiment with optimal a=2.8 nmol^{-1} s g and YIBs-S2007_adj. Blue (red) patches indicate the regions where damage in YIBs-LMA_B2017 with optimal a are weaker (stronger) than YIBs-S2007_adj. Experiments are described in Table 1.

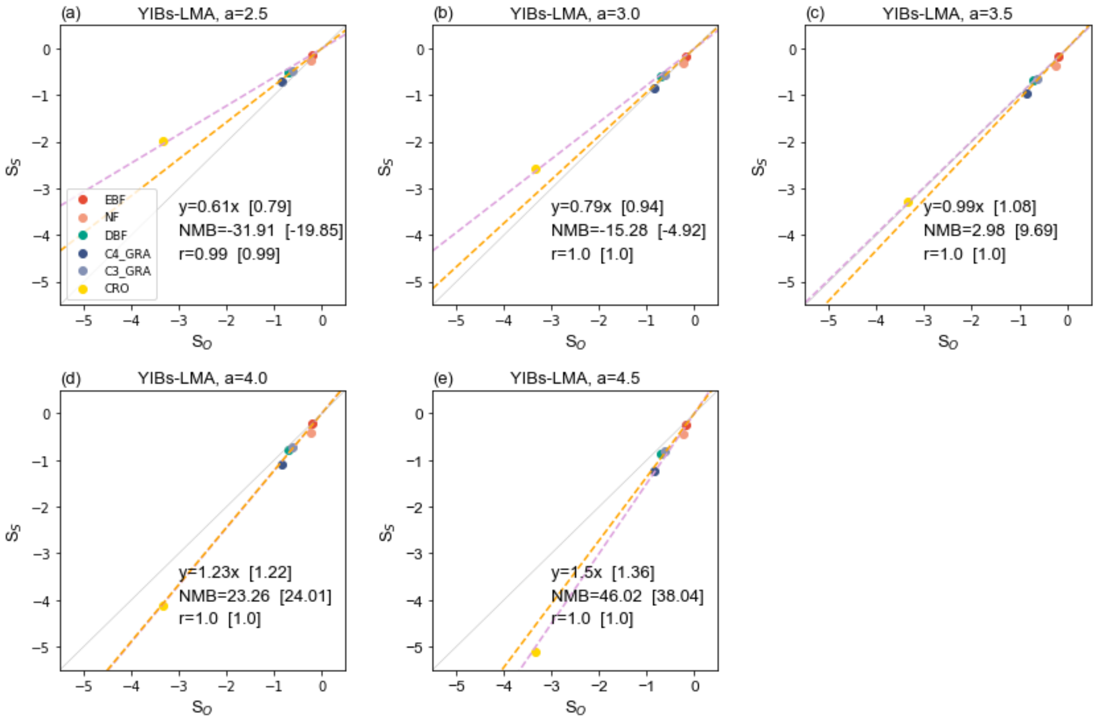

Figure S8. Supplementary calibrations excluding CRO are shown as orange dashed lines. Original calibration in Fig. 3 and 1:1 fitting are shown as dashed pink and light grey, respectively. The new slope, NMB, and r are recalculated and noted in square brackets.

Supplementary References

Alonso, R., Elvira, S., Inclan, R., and Bermejo, V.: Responses of Aleppo pine to ozone, in: Dev Environm Sci, Developments in Environmental Science, 211-230, 2003.

Alonso, R., Elvira, S., Gonzalez-Fernandez, I., Calvete, H., Garcia-Gomez, H., and Bermejo, V.: Drought stress does not protect Quercus ilex L. from ozone effects: results from a comparative study of two subspecies differing in ozone sensitivity, Plant Biology, 16, 375-384, 10.1111/plb.12073, 2014.

Assis, P. I. L. S., Alonso, R., Meirelles, S. T., and Moraes, R. M.: DO3SE model applicability and O-3 flux performance compared to AOT40 for an O-3-sensitive tropical tree species (Psidium guajava L. 'Paluma'), Environ Sci Pollut R, 22, 10873-10881, 10.1007/s11356-015-4293-1, 2015.

Braun, S. and Fluckiger, W.: EFFECTS OF AMBIENT OZONE ON SEEDLINGS OF FAGUS-SYLVATICA L AND PICEA-ABIES (L) KARST, New Phytol, 129, 33-44, 10.1111/j.1469-8137.1995.tb03007.x, 1995.

Buker, P., Feng, Z., Uddling, J., Briolat, A., Alonso, R., Braun, S., Elvira, S., Gerosa, G., Karlsson, P. E., Le Thiec, D., Marzuoli, R., Mills, G., Oksanen, E., Wieser, G., Wilkinson, M., and Emberson, L. D.: New flux based dose-response relationships for ozone for European forest tree species, Environ Pollut, 206, 163-174, 10.1016/j.envpol.2015.06.033, 2015.

Calatayud, V., Cervero, J., Calvo, E., Garcia-Breijo, F.-J., Reig-Arminana, J., and Jose Sanz, M.: Responses of evergreen and deciduous Quercus species to enhanced ozone levels, Environ Pollut, 159, 55-63, 10.1016/j.envpol.2010.09.024, 2011.

CLRTAP: The UNECE Convention on Long-range Transboundary Air Pollution, Manual on Methodologies and Criteria for Modelling and Mapping Critical Loads and Levels and Air Pollution Effects, Risks and Trends: Chapter III Mapping Critical Levels for Vegetation, 2017.

Dixon, M., Le Thiec, D., and Garrec, J. P.: Reactions of Norway spruce and beech trees to 2 years of ozone exposure and episodic drought, Environ Exp Bot, 40, 77-91, 10.1016/s0098-8472(98)00023-9, 1998.

Elvira, S., Alonso, R., and Gimeno, B. S.: Simulation of stomatal conductance for Aleppo pine to estimate its ozone uptake, Environ Pollut, 146, 617-623, 10.1016/j.envpol.2006.08.008, 2007.

Feng, Z. Z., Buker, P., Pleijel, H., Emberson, L., Karlsson, P. E., and Uddling, J.: A unifying explanation for variation in ozone sensitivity among woody plants, Global Change Biol, 24, 78-84, 10.1111/gcb.13824, 2018.

Gimeno, B. S., Bermejo, V., Sanz, J., de la Torre, D., and Elvira, S.: Growth response to ozone of annual species from Mediterranean pastures, Environ Pollut, 132, 297-306, 10.1016/j.envpol.2004.04.022, 2004a.

Gimeno, B. S., Bermejo, V., Sanz, J., De la Torre, D., and Gil, J. M.: Assessment of the effects of ozone exposure and plant competition on the reproductive ability of three therophytic clover species from Iberian pastures, Atmos Environ, 38, 2295-2303, 10.1016/j.atmosenv.2003.10.062, 2004b.

Harmens, H., Hayes, F., Mills, G., Sharps, K., Osborne, S., and Pleijel, H.: Wheat yield responses to stomatal uptake of ozone: Peak vs rising background ozone conditions, Atmos Environ, 173, 1-5, 2018.

Hayes, F., Williamson, J., and Mills, G.: Ozone pollution affects flower numbers and timing in a simulated BAP priority calcareous grassland community, Environ Pollut, 163, 40-47, 10.1016/j.envpol.2011.12.032, 2012.

Hayes, F., Harmens, H., Sharps, K., and Radbourne, A.: Ozone dose-response relationships for tropical crops reveal potential threat to legume and wheat production, but not to millets, Scientific African, 9, 2020.

Hayes, F., Mills, G., Harmens, H., and Wyness, K.: Within season and carry-over effects following exposure of grassland species mixtures to increasing background ozone, Environ Pollut, 159, 2420-2426, 10.1016/j.envpol.2011.06.034, 2011.

Hewitt, D. K. L., Mills, G., Hayes, F., Wilkinson, S., and Davies, W.: Highlighting the threat from current and near-future ozone pollution to clover in pasture, Environ Pollut, 189, 111-117, 10.1016/j.envpol.2014.02.033, 2014.

Hoshika, Y., Moura, B., and Paoletti, E.: Ozone risk assessment in three oak species as affected by soil water availability, Environ Sci Pollut R, 25, 8125-8136, 2018.

Hu, E., Gao, F., Xin, Y., Jia, H., Li, K., Hu, J., and Feng, Z.: Concentration- and flux-based ozone dose–response relationships for five poplar clones grown in North China, Environ Pollut, 207, 21-30, https://doi.org/10.1016/j.envpol.2015.08.034, 2015.

Karlsson, P. E., Uddling, J., Skarby, L., Wallin, G., and Sellden, G.: Impact of ozone on the growth of birch (Betula pendula) saplings, Environ Pollut, 124, 485-495, 10.1016/s0269-7491(03)00010-1, 2003.

Karlsson, P. E., Uddling, J., Braun, S., Broadmeadow, M., Elvira, S., Gimeno, B. S., Le Thiec, D., Oksanen, E., Vandermeiren, K., Wilkinson, M., and Emberson, L.: New critical levels for ozone effects on young trees based on AOT40 and simulated cumulative leaf uptake of ozone, Atmos Environ, 38, 2283-2294, 10.1016/j.atmosenv.2004.01.027, 2004.

Marzuoli, R., Monga, R., Finco, A., and Gerosa, G.: Biomass and physiological responses of Quercus robur (L.) young trees during 2 years of treatments with different levels of ozone and nitrogen wet deposition, Trees-Struct Funct, 30, 1995-2010, 10.1007/s00468-016-1427-0, 2016.

Marzuoli, R., Bussotti, F., Calatayud, V., Calvo, E., Alonso, R., Bermejo, V., Pollastrini, M., Monga, R., and Gerosa, G.: Dose-response relationships for ozone effect on the growth of deciduous broadleaf oaks in mediterranean environment, Atmos Environ, 190, 331-341, 10.1016/j.atmosenv.2018.07.053, 2018.

Medlyn, B. E., Badeck, F. W., De Pury, D. G. G., Barton, C. V. M., Broadmeadow, M., Ceulemans, R., De Angelis, P., Forstreuter, M., Jach, M. E., Kellomaki, S., Laitat, E., Marek, M., Philippot, S., Rey, A., Strassemeyer, J., Laitinen, K., Liozon, R., Portier, B., Roberntz, P., Wang, K., and Jarvis, P. G.: Effects of elevated CO2 on photosynthesis in European forest species: a meta-analysis of model parameters, Plant Cell Environ, 22, 1475-1495, 10.1046/j.1365-3040.1999.00523.x, 1999.

Oliver, R. J., Mercado, L. M., Sitch, S., Simpson, D., Medlyn, B. E., Lin, Y. S., and Folberth, G. A.: Large but decreasing effect of ozone on the European carbon sink, Biogeosciences, 15, 4245-4269, 10.5194/bg-15-4245-2018, 2018.

Ottosson, S., Wallin, G., Skarby, L., Karlsson, P. E., Medin, E. L., Rantfors, M., Pleijel, H., and Sellden, G.: Four years of ozone exposure at high or low phosphorus reduced biomass in Norway spruce, Trees-Struct Funct, 17, 299-307, 10.1007/s00468-002-0239-6, 2003.

Peng, J., Shang, B., Xu, Y., Feng, Z., and Calatayud, V.: Effects of ozone on maize (Zea mays L.) photosynthetic physiology, biomass and yield components based on exposure- and flux-response relationships, Environ Pollut, 256, 10.1016/j.envpol.2019.113466, 2020.

Peng, J. L., Shang, B., Xu, Y. S., Feng, Z. Z., Pleijel, H., and Calatayud, V.: Ozone exposure- and flux-yield response relationships for maize, Environ Pollut, 252, 1-7, 2019.

Sanz, J., Bermejo, V., Gimeno, B. S., Elvira, S., and Alonso, R.: Ozone sensitivity of the Mediterranean terophyte Trifolium striatum is modulated by soil nitrogen content, Atmos Environ, 41, 8952-8962, 10.1016/j.atmosenv.2007.08.016, 2007.

Sanz, J., Muntifering, R. B., Bermejo, V., Gimeno, B. S., and Elvira, S.: Ozone and increased nitrogen supply effects on the yield and nutritive quality of Trifolium subterraneum, Atmos Environ, 39, 5899-5907, 10.1016/j.atmosenv.2005.06.022, 2005.

Sanz, J., Gonzalez-Fernandez, I., Elvira, S., Muntifering, R., Alonso, R., and Bermejo-Bermejo, V.: Setting ozone critical levels for annual Mediterranean pasture species: Combined analysiS of open-top chamber experiments, Sci Total Environ, 571, 670-679, 10.1016/j.scitotenv.2016.07.035, 2016.

Sanz, J., Gonzalez-Fernandez, I., Calvete-Sogo, H., Lin, J. S., Alonso, R., Muntifering, R., and Bermejo, V.: Ozone and nitrogen effects on yield and nutritive quality of the annual legume Trifolium cherleri, Atmos Environ, 94, 765-772, 10.1016/j.atmosenv.2014.06.001, 2014.

Uddling, J., Pleijel, H., and Karlsson, P. E.: Measuring and modelling leaf diffusive conductance in juvenile silver birch, Betula pendula, Trees-Struct Funct, 18, 686-695, 2004.

Wagg, S., Mills, G., Hayes, F., Wilkinson, S., Cooper, D., and Davies, W. J.: Reduced soil water availability did not protect two competing grassland species from the negative effects of increasing background ozone, Environ Pollut, 165, 91-99, 10.1016/j.envpol.2012.02.010, 2012.

Wyness, K., Mills, G., Jones, L., Barnes, J. D., and Jones, D. L.: Enhanced nitrogen deposition exacerbates the negative effect of increasing background ozone in Dactylis glomerata, but not Ranunculus acris, Environ Pollut, 159, 2493-2499, 10.1016/j.envpol.2011.06.022, 2011.

Zhang, W. W., Feng, Z. Z., Wang, X. K., Liu, X. B., and Hu, E. Z.: Quantification of ozone exposure- and stomatal uptake-yield response relationships for soybean in Northeast China, Sci Total Environ, 599, 710-720, 10.1016/j.scitotenv.2017.04.231, 2017.